LeRoy D. Dickson Glenn T. Sincerbox Albert D. Wolfheimer

Holography in the IBM 3687 Supermarket Scanner

The IBM 3687 Supermarket Scanner is described, with emphasis on the holographic deflector disk used to create the scan pattern. The scanner exploits the functional advantages of holography to create a dense, multiple-focal-plane scan pattern with small spot size and large depth of field. The optical design of the holographic disk is discussed and basic disk fabrication concepts are introduced.

Introduction

In 1973 the Uniform Product Code Council announced the Universal Product Code (UPC), which would soon appear on grocery items in the supermarket. Shortly thereafter, IBM announced the 3666, the first laser scanner designed to read the UPC bar code symbol. Since that time the number of grocery items bearing UPC symbols has increased to the point where nearly all grocery items bear the now-familiar bar code.

In the original concept, UPC label readers were basically designed to be "bottom readers." That is, the items were to be brought across the scan window with the label down against the window, or nearly so. To allow for unusual package shapes, it was specified that label readers should have a depth of field of 12.5 mm (0.5 in.), a basic requirement which persists to this day. It is important to note that this relatively modest depth-of-field requirement is compatible with the further requirement that the scanner be able to read labels with bar widths and space widths on the order of 0.2 mm. Laser scanners can easily meet both of these requirements.

The basic concepts of a laser-scanning UPC reader are now fairly familiar. As an item approaches the scan window it breaks an item sensor beam path, causing the opening of an internal shutter to allow the scanning laser beam to appear at the window. When the scanning beam sweeps across the UPC bar code, the reflected laser light is sensed by an internal photodetector that converts the optical signal

to an electrical signal, which is then digitized and decoded. The computer identifies the item from this decoded signal and transmits its description and price to the checker display and to the customer receipt. For further discussion of scanning and the UPC code, interested readers are referred to Refs. [1-4].

During the past eight years, scanner design has diverged from the original bottom scanning concept. The objective of the changes was to minimize the constraints on the operator so that throughput and productivity could be increased. For example, in the original 3666 scanner the depth of field was sufficient to allow the operator merely to tilt the items toward the window rather than placing them flat on the window [see Fig. 1(a)]. An extension of this tilted reading concept is a forward-looking scanner which tilts the beam, thereby allowing the item to be read in an upright position [Fig. 1(b)]. Reading a tilted item obviously requires more depth of field; however, a forward-looking tilted-beam scanner requires an even greater depth of field.

As scanners have evolved away from bottom scanning, the depth-of-field requirements have increased dramatically beyond that originally specified. However, the minimum bar widths that must be read are still on the order of 0.2 mm. A cursory analysis of the properties of a Gaussian laser beam reveals that typical depths of field of 150 mm are incompatible with the ability to consistently read a bar/space width of 0.2 mm, especially if the label is of low to medium

Copyright 1982 by International Business Machines Corporation. Copying is permitted without payment of royalty provided that (1) each reproduction is done without alteration and (2) the *Journal* reference and IBM copyright notice are included on the first page. The title and abstract may be used without further permission in computer-based and other information-service systems. Permission to republish other excerpts should be obtained from the Editor.

contrast. Newer scanner designs have carried the evolution one step further by projecting the tilted scan pattern toward the sides of the package, as well as toward the front, providing a "wraparound" scan pattern. This feature is particularly advantageous since it allows a greater freedom in the orientation of the package as it crosses the scan window. However, such designs further aggravate the depth-of-field problem.

Scanner requirements and design

The major goal in the design of the 3687 was to find a design approach which would allow us to take advantage of the benefits of the tilted wraparound scan pattern without having to accept shortcomings inherent to the large depth of field required. In essence, the object was to achieve a large depth of field (>150 mm) with a small spot size (<0.25 mm) throughout the full depth of field, and to accomplish this within the limits of a Class I laser product, as defined by the BRH laser standard of the USFDA. The scanner was to be capable of front, side, or bottom reading. Furthermore, the box had to be small in order to be compatible with a variety of checkstand furniture, and the scan surface should be smooth to simplify item handling while scanning. The holographic deflector was the key scanner element which allowed us to achieve this objective.

In order to achieve a large depth of field with a small spot size, one should project multiple focal surfaces out of the scan window. That is, instead of using a few long scan lines with a single focal length, one uses many short scan lines with differing focal lengths. In this manner, one set of short scan lines can be focused near the scan window, while another set can be focused further from the window. Each set would have only a moderate depth of field, but with a small spot size throughout. The combined depth of field would be quite large, without any sacrifice in spot size.

The multiple-scan-line concept and the requirement for a smooth scan surface meant that the scan pattern had to exit through a rectangular window (9.5 × 15.25 cm) and that the scan pattern would be spatially very dense both at the window and in the forward projection direction. This results in rapid label acquisition; *i.e.*, the label is read quickly after breaking the item sensor. One advantage of rapid label acquisition is that the audible response tone (positive scan feedback) occurs sooner, allowing a faster operating pace. A second advantage is that the shutter closes sooner, reducing the time of exposure to laser light, a key factor in our effort to achieve a Class I scanner. The Class I requirement also meant that the internal light collection paths had to be short and light collection efficiencies high to maximize the returned laser light and minimize the required laser power.

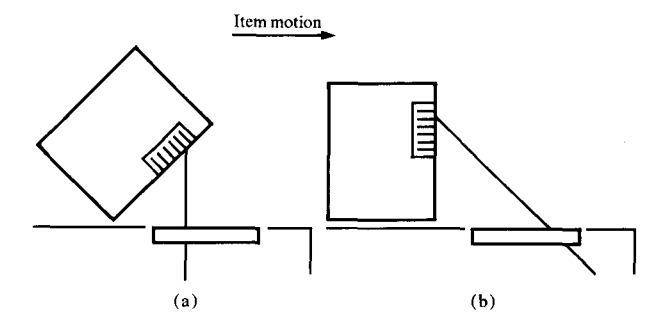


Figure 1 Depth of focus required for (a) a tilted package and (b) a tilted beam in a label-scanning system.

All of the above requirements dictate the use of a multi-faceted rotating element for deflecting the laser beam. Furthermore, the individual facets of the rotating element must have different sizes, tilt angles, and focal lengths. The variation in facet size allows generation of fairly complex scan patterns while maintaining uniform light collection throughout the scan region.

In theory, all of the above requirements could be met using a complex multi-faceted rotating mirror. However, even if it were practical to make such a device, the cost would be prohibitive. Therefore, we decided to use a holographic disk as our laser deflector. Such a device, in addition to meeting all of our design requirements, provided design flexibility during the development of the scanner.

Scan pattern

A computer simulation program [5] was used to determine the optimum scan pattern within the limitations established by our design objectives. Various combinations of multiple interlaced Xs and horizontal and diagonal lines were examined within the confines of the 9.5×15.25 -cm window. Several combinations of exit beam angles were also examined. The program simulated a typical distribution of label sizes, orientations, locations, contrasts, velocities, pass angles, and tilts. The scanner parameters included in the simulation were scan angle in the window plane, elevation angle, spot size, spot ellipticity, depth of field, and light collection efficiency.

The resulting optimized scan pattern on the window plane is shown in Fig. 2(a). The same pattern projected onto a vertical plane near the item sensor beam path is shown in Fig. 2(b). The horizontal lines in Fig. 2(a) project forward at \approx 45° in elevation to read vertical bar labels on the fronts or bottoms of packages. The X lines project forward and inward along the scan line to read horizontal bar labels on the fronts, bottoms, or sides of packages. The two pairs of outer 45° skew lines are similar to the horizontal lines, but

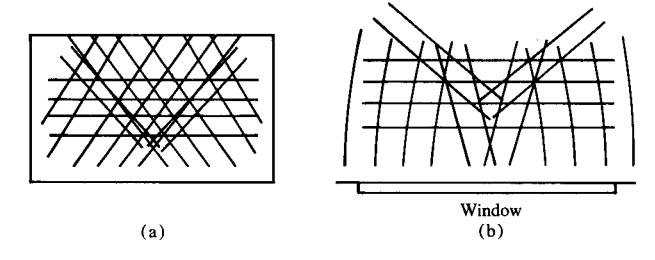


Figure 2 Scan pattern (a) on window and (b) on vertical plane in front of window.

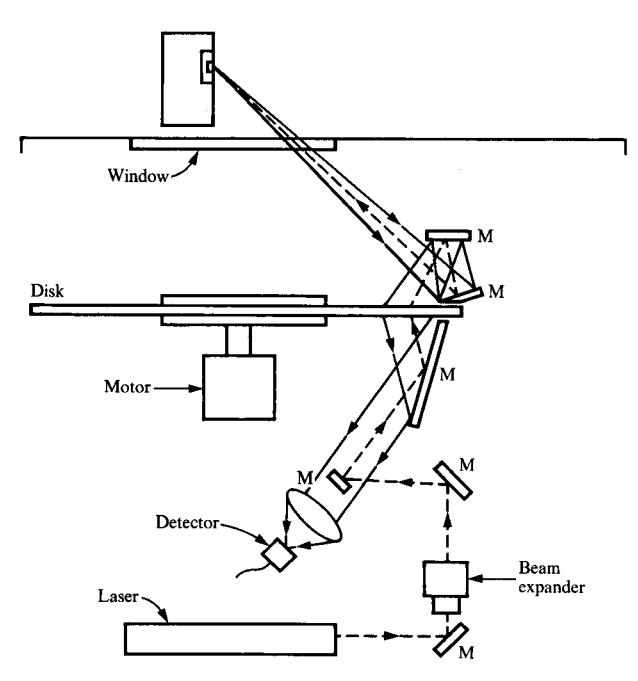


Figure 3 Scanner optical design; mirrors are designated by a capital letter \mathbf{M} .

project forward and inward (perpendicular to the scan line) at an elevation angle of \approx 45° to read vertical bar labels on the sides and bottoms of packages.

The density of the scan pattern is evident in the figure. Labels on the fronts or sides of packages are generally read shortly after the item sensor beam path is broken and before the package actually reaches the scan window. Labels on the bottom of packages are generally read in the leading half of the scan window.

The scan pattern is created by selecting the proper deflection angles and focal lengths for the individual facets of the holographic disk, and by combining these with the proper beam folding mirror angles. Design of the mirror subassembly was a fairly complex task since the scanner operates in a retroreflective mode (see Fig. 3). That is, the collected light returns to the detector along the same path as the outgoing beam. Therefore, the mirror design must account for the light collection cone of the returning beam as well as the scan length of the outgoing beam. Each mirror must be big enough to avoid truncating the return beam but small enough to avoid obstructing the light path to adjacent mirrors. Since there are eleven mirrors in a fairly compact scan box, this was no mean task. An APL program was written to simulate the entire mirror subassembly in combinations with the holographic disk. It checked the precise location, size, shape, and tilt angle of all eleven mirrors and calculated the light collection back to the disk for a given combination of disk facet sizes, deflection angles, and focal lengths.

• Scanner optical elements

The entire optical system is shown in Fig. 3. The outgoing expanded laser beam strikes the disk at a 22° angle of incidence (discussed in the next section). The rotating holographic disk diffracts and deflects the beam, creating multiple scan lines that are brought together at the scan window by the folding mirror subassembly. Some of the diffuse light is reflected back along the path of the outgoing beam to the holographic disk, where it is collimated and directed back toward the aspheric collection lens that focuses the light onto the detector.

The light collection efficiency of an individual facet of the holographic disk is a function of the facet area projected normal to the outgoing laser beam, and of the distance from the facet to the focal point of the beam. Since both the path length to the window and the elevation angle of the diffracted beam vary from facet to facet, the facets tend to have widely varying light collection efficiencies. However, the holographic disk allows us to easily vary facet widths to equalize these efficiencies, thus significantly reducing the overall signal range to be handled by the electronics. This capability also permits a great deal of flexibility in the design of the scanner.

In the actual disk, the facet widths vary from 14 to 25.5° in order to equalize the light collection efficiency for all facets. The light collection solid angle for all facets is $\approx 5 \times 10^{-3}$ sr (steradians).

The laser is a 1.5-mW polarized HeNe laser (633 nm). The polarization direction is selected to minimize reflection losses for the beam at the scanner window surfaces. A photomultiplier is used for the detector to maximize the signal-to-noise ratio.

The holographic disk

The concept of holographic scanning was first proposed in 1967 by I. Cindrich [6]. Since that time, others have proposed a variety of scanning systems utilizing holography [7, 8]. Where volume production costs are a major concern, the ability to reproduce the deflecting element at a reasonable cost is a key factor in determining which scanner design approach to use. The disk design allows for relative ease of manufacturing through the use of a master/copy process. The master disk is made on silver halide material at 633 nm; copies are made on dichromated gelatin (DCG) at 488 nm.

• Optical design

The 3687 holographic disk design is shown in Fig. 4. There are 21 facets; 20 are used to generate the 20-line scan pattern, while the remaining facet scans an internal diagnostic label. The variation in facet width previously discussed is apparent in the figure. Each facet is a separate hologram with a unique combination of focal length F, skew angle θ_s , and elevation angle B. Each facet deflects and focuses the outgoing beam, and collects and collimates a portion of the diffuse light reflected from the label. As the disk rotates, the beam sweeps across the scan window, creating the entire scan pattern in one revolution of the disk.

The disk diameter is 195 mm; the facet length is 50 mm, while the facet width varies from 10 (for the diagnostic facet) to 25.5°. The disk itself is actually a sandwich consisting of two identical glass disks with the holographic medium sandwiched between them.

The diffracted output beam f-numbers range from 200 to 300. The input reconstruction beam is an expanded collimated beam entering the disk at a radial distance R=72 mm from the center and at an angle of incidence (defined as the angle between the normal and the input beam) equal to 22° . This is a departure from conventional practice, where the collimated beam enters the disk normal to the disk surface. The conventional approach has the advantage of being aberration-free during scanning; however, there are a number of significant advantages to the tilted collimated-beam approach which more than compensate for the small amount of aberration introduced.

The use of a tilted collimated reference beam for a holographic disk with focusing facets was a significant departure from conventional practice. It was the major factor that allowed us to fully exploit the unique advantages of the holographic deflector disk. The reasoning behind this may not be obvious to the reader; therefore, we discuss the technical aspects of this approach in detail.

To avoid aberrations during reconstruction in conventional holography, the playback geometry should be identi-

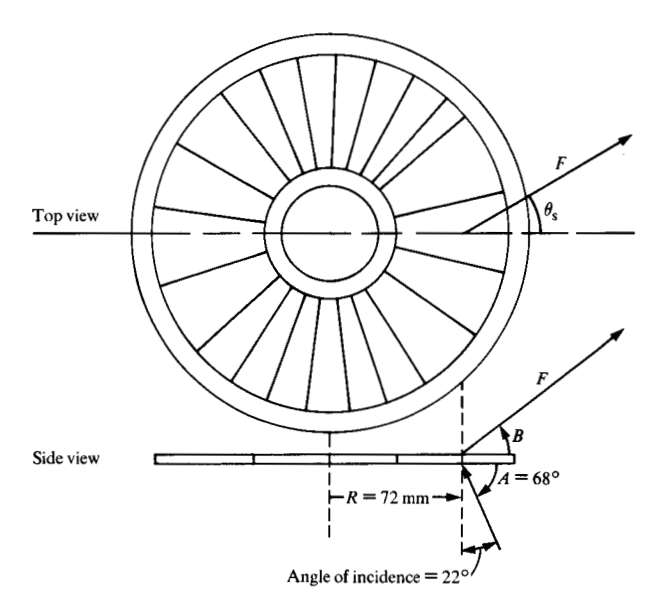


Figure 4 Disk design parameters.

cal to either the recording geometry or its conjugate. In a holographic disk, this will occur, in general, for the full range of facet rotation only if the reference/reconstruction source converges to, or appears to diverge from, a point on the rotational axis of the disk. The collimated beam normal to the disk surface (parallel to the disk rotational axis) is a special but commonly occurring example of this geometry.

A major disadvantage of the normal beam geometry, when using a wet-process medium such as DCG, is that it introduces a large tilt angle to the Bragg surfaces in the recording media [α in Figs. 5(a) and (b)]. DCG retains some residual swell after processing so that the thickness of the playback medium is greater than that of the recording medium. This produces a shift in Bragg surface tilt $(\Delta \alpha)$. The larger the original Bragg surface tilt, the greater the shift in α after processing. Such a shift means that the angle of incidence which produces maximum diffraction efficiency no longer coincides with the original reference/reconstruction beam angle. The net effect is a loss in diffraction efficiency. The tilted reference beam angle minimizes this problem by reducing the tilt angle of the Bragg surfaces. In the limit where A = B, the residual gel swell has no effect on the tilt of the Bragg surfaces since they are normal to the gel surface [Figs. 5(c) and (d)].

Another disadvantage of the conventional normal collimated reference beam design is that it limits the usable range of the elevation angle B. In the scanner it is desirable to have a large range of diffracted beam elevation angle in

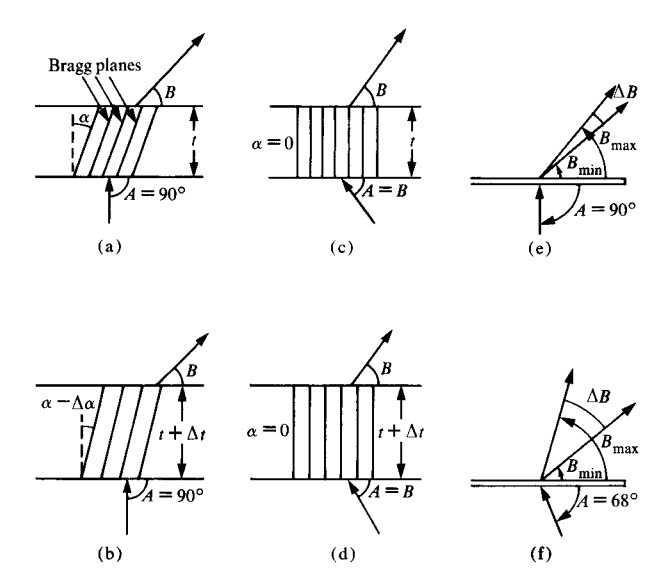


Figure 5 Bragg planes (a) before and (b) after processing with $A = 90^{\circ}$. Bragg planes (c) before and (d) after processing with A = B. Effect of angle A on the usable range of angle B for A equal to (e) 90° and (f) 68° .

order to be able to spatially separate the various groups of scan lines within a reasonably short distance from the disk. This allows obstruction-free beam paths in a compact mirror subassembly design.

The effect of the reference beam input angle A on the elevation angle range ΔB can be seen in Figs. 5(e) and (f). The minimum elevation angle $B_{\min} \approx 40^{\circ}$. Other requirements in the scanner dictated the use of an S-polarized input beam. Thus, for elevation angles <40°, the Fresnel reflection losses at the disk surface become too large.

The maximum elevation angle $B_{\rm max}$ is established by the combined requirements of a relatively thin holographic medium and the need to satisfy the Bragg diffraction condition. These requirements set an upper limit on the sum (A+B), $\approx 140^{\circ}$. If $A=90^{\circ}$, $B_{\rm max}=50^{\circ}$ and $\Delta B=10^{\circ}$. On the other hand, if $A=68^{\circ}$, $B_{\rm max}=72^{\circ}$ and $\Delta B=32^{\circ}$. The difference is clearly seen in Figs. 5(e) and (f).

A further disadvantage of the normal collimated reference beam design is that the diffracted beam is foreshortened in the radial direction leading to an asymmetric spot at the focal plane. A tilted reference beam will reduce this problem. Obviously, foreshortening can only be completely eliminated in the single case where A = B.

One practical advantage for the tilted reference beam is the reduced sensitivity to disk wobble (oscillations about an axis normal to the rotational axis of the disk and lying in the plane of the disk). If we assume that the incident beam is fixed in space in the scanner, wobble will cause A and B to vary. However, the angle of interest in the scanner is the total deviation angle (A + B). It is a simple matter to show, using the grating equation, that $\Delta(A + B)/\Delta A$ approaches a minimum as A approaches B. Therefore, the effect of wobble in the tilted beam design is less than that in the normal beam design.

The tilted collimated reference/reconstruction beam design has one final advantage worth discussing. It can be shown that a tilted collimated input beam provides a scan angle multiplication factor (relative to an untilted collimated input beam). A precise determination of the multiplication factor requires utilization of an APL program; however, a relatively simple scan angle equation (1) gives this factor in a straightforward manner with an error of <1% (due to the interdependence of B and the disk rotation angle).

If we let $\phi_{\rm rot}$ be the rotational angle of the disk and $\phi_{\rm scan}$ be the scan angle of the deflected beam,

$$\phi_{\text{scan}} = \phi_{\text{rot}} \left(\frac{R}{F} \cos \theta_{\text{s}} + \cos A + \cos B \right), \tag{1}$$

where R=72 mm in our disk and F, B, and θ_s are the focal length, elevation angle, and skew angle as shown in Fig. 4. θ_s is the nominal design skew angle of the facet, *i.e.*, the skew angle when the facet is centered on the input beam. Note that use of the grating equation reduces (1) to

$$\phi_{\text{scan}} = \phi_{\text{rot}} \left(\frac{R}{F} \cos \theta_{\text{s}} + \frac{\lambda}{d} \right),$$

where λ is the wavelength and d is the surface fringe spacing.

The multiplication effect of the tilted collimated input beam is due to the $\cos A$ term in (1); for normal incidence, this term goes to zero.

As an example of the effect of the tilt, consider a typical facet with F=350 mm, $\theta_s=40^\circ$, $B=66^\circ$, and R=72 mm. For normal incidence, $\phi_{\rm scan}=0.564\phi_{\rm rot}$, while for a tilted 68° beam, $\phi_{\rm scan}=0.939\phi_{\rm rot}$. The relative multiplication factor obtained by using the tilted beam is 1.66. This is significant because it implies that a given facet can be closer to the window for a given scan length and facet width. The effect is somewhat greater than indicated since a facet closer to the window would necessarily have a shorter focal length. This would, in turn, tend to further increase $\phi_{\rm scan}$ for a given $\phi_{\rm rot}$, as seen from Eq. (1). Overall, the tilt angle in our disk resulted in an average multiplication factor of \approx 1.6. Thus, for a given total scan length, the disk is closer to the window

by a factor of 1.6 for the tilted vs. untilted input beam, and the light collection efficiency is better by a factor of $(1.6)^2$. This is a major factor in our ability to read well while remaining within the Class I laser-power limits.

Although there are numerous advantages to the tilted collimated beam design, aberrations are introduced by such a design. The major aberration is the astigmatism introduced as the disk rotates away from the nominal position where the input beam strikes the center of the facet, which increases as the facet rotates further from this nominal position. However, all of our facets have a relatively narrow angular width; thus, the amount of astigmatism introduced is fairly small, even at the ends of the scan lines.

To examine the effects of astigmatism, the previously mentioned ray-tracing program was expanded to treat a bundle of rays in order to provide information in the form of geometrical spot diagrams. The effect of varying record and playback parameters (wavefront curvature, angle of incidence wavelength, etc.) were examined, and the resulting aberrations determined. Figure 6 shows the typical effect of a tilted collimated reference and a playback beam. Each row represents the spot diagrams at different positions along the same scan line at tilt angles of (a) 68, (b) 78, and (c) 88°. As expected, the aberrations become more pronounced as the tilt increases. Note the magnification in the scan length (width of individual spot patterns) introduced with increasing tilt. The full angular width for this facet is not required; thus, at 68° tilt the residual aberration is <10%.

If one does not need or desire the scan angle multiplication feature but would like to use some or all of the remaining properties of the tilted beam, a tilted reference beam converging to a point on the rotational axis should be used instead of a collimated beam. In this case, there is no scan angle multiplication factor, and the scanning spot is completely free of aberrations.

• Fabrication

The DCG holographic disk is made using a holographic contact copy process. A silver halide master holographic disk is placed in contact with an unexposed DCG disk. The master disk is then illuminated at the appropriate angle by an expanded beam from an Ar laser. The diffraction efficiency of the master disk is relatively low, so that light leaves the disk as two beams of nearly equal intensity, the diffracted beam and the reference beam. These act as object and reference beams, respectively, for the underlying DCG disk. The master disk thus acts as a source of two wavefronts for the holographic rerecording in the DGC disk of each facet of the master disk.

Each master holographic facet is recorded in a conventional manner using a HeNe laser and a vibration isolated

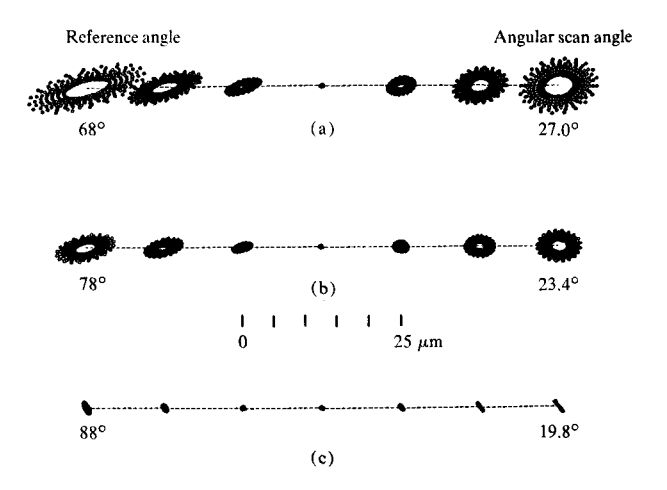


Figure 6 Geometrical spot patterns along a scan line for three different inclination angles of the reference/playback beam; tilt angle, angular scan angle (in degrees): (a) 68, 27.0; (b) 78, 23.4; and (c) 88, 19.8. Note the magnification in the scan length with increasing inclination.

optical table. The facets are cut to size and mounted on a disk substrate to form the master disk. In the copying process, an index-matching fluid is used between the silver halide holographic master and the DCG-coated copy disk. The angle of illumination of the laser is modified for the change in wavelength (633 nm to 488 nm). Each facet is exposed individually in a step-and-repeat process with suitable masking to prevent exposure of adjacent facet areas. Since the master disk is made at 633 nm, and the DCG copy disk is to be used in the scanner at the same wavelength, no chromatic aberration is introduced, even though the intermediate copy wavelength is different [9].

DCG was selected as the copy disk holographic medium because of the high diffraction efficiency obtainable in a relatively thin emulsion. Other media are capable of yielding high diffraction efficiencies, but only with much thicker emulsions. Thicker emulsions are very sensitive to the Bragg angle; the diffraction efficiency falls off rapidly on either side of the optimum reconstruction angle. This causes the diffraction efficiency to vary during scanning and also severely restricts manufacturing tolerances. In a scanning application such as the 3687, the thinner the holographic medium, the better, so long as high first-order diffraction efficiency is achieved.

There are numerous articles which discuss the coating, sensitizing, exposing, and processing of DCG [10-12]; thus, we do not discuss them in detail here. Our objective was to establish a process that would provide consistent results in order to obtain high manufacturing yields. The key to accomplishing this was the development of an overall process that yielded a consistent amount of residual post-processing

gelatin swell. This residual gelatin swell causes a shifting of the Bragg surfaces, with a resultant decrease in diffraction efficiency for a fixed reconstruction beam angle [see Figs. 5(a) and (b)]. There are no methods for eliminating this swell that are practical from a manufacturing standpoint. However, if the swell is predictable and consistent, it can be compensated for in the copy process by reducing the calculated angle of incidence of the copy beam. This increases the Bragg surface tilt angle α . The post-processing residual swell acts to decrease the tilt angle, thereby returning α to the desired value.

After the copy disk is exposed and processed, several millimeters of gelatin are stripped from the outer and inner edges and it is sealed with a glass cover disk to provide protection from moisture. A metal hub is then bonded to the inner diameter of the disk and the disk is dynamically balanced. The complete disk is checked for optical performance in an automated tester.

◆ Analysis

Testing of a large number of DCG disks has shown that in all cases the copy disk is a faithful reproduction of the master disk in terms of deflection angles, focal lengths, and spot sizes. Diffraction efficiencies run as high as 80%, with the 20% loss being attributed to Fresnel reflections at the glass surfaces, absorption and scattering in the gelatin, and a very small amount of zero order beam. Optical tests performed on the disk following prolonged exposure to temperature humidity cycling indicate no degradation in diffraction efficiency or overall optical performance. In addition, no printout effects have been observed due to extensive exposure to ultraviolet light.

Summary

We have described the optical system and holographic deflector that have been designed and fabricated for use in the IBM 3687 supermarket scanner. Using a multi-facet configuration, the functional advantages of holography are exploited to simultaneously deflect and focus the scanning beam and then to collect and collimate the diffuse light scattered by the UPC label. A high-density scan pattern, which has a depth of field of at least 150 mm and a 180° wraparound scan, is generated. This is accomplished by providing individual facets with unique scan directions and focal lengths, and by combining each with an appropriate set of mirrors. Holographic disks are mass-produced in a master/copy process that uses silver halide emulsions and

dichromated gelatin. The result is an environmentally stable highly uniform disk of high diffraction efficiency, an overall optical system with good signal-to-noise ratio, and a scanner system with excellent product throughput. The scanner meets all of our original design objectives and is relatively compact.

The entire optical system for creating the high-density, multiple-focal-plane scan pattern fits in a compact optical cavity. The ability to accomplish this can be attributed to the unique optical properties of the holographic scanning disk.

References and note

- L. D. Dickson, "Lasers in Supermarket Point-of-Sale Systems," Code and Symbols 2, No. 1, 5 (1976).
- A. Hildebrand, "Reading the Supermarket Code," Laser Focus 10, 10 (1974).
- P. W. Wu and J. C. Tandon, "Omnidirectional Laser Scanner for Supermarkets," Opt. Eng. 20, 123 (1981).
- D. Savir and G. J. Laurer, "The Characteristics and Decodability of the Universal Product Code," IBM Syst. J. 14, 16 (1975).
- The original program was devised by Joel Lehmann of North Carolina State University (NCSU), Raleigh, NC. This program was later expanded and improved by Stephen Campbell of NCSU and Scott Fortenberry of IBM's Communication Products Division, Raleigh, NC.
- I. Cindrich, "Image Scanning by Rotation of a Hologram," Appl. Opt. 6, 1531 (1967).
- D. McMahon, A. Franklin, and J. Thaxten, "Light Beam Deflection Using Holographic Scanning Techniques," Appl. Opt. 8, 399 (1969).
- R. V. Pole and H. P. Wollenmann, "Holographic Laser Beam Deflector," Appl. Opt. 14, No. 4, 976 (1975).
- L. H. Lin and E. T. Doherty, "Efficient and Aberration-Free Wavefront Reconstruction Form Holograms Illuminated at Wavelengths Differing from the Forming Wavelength," Appl. Opt. 10, 1314 (1971).
- T. A. Shankoff, "Phase Holograms in Dichromated Gelatin," Appl. Opt. 7, 2101 (1968).
- B. J. Chang and C. D. Leonard, "Dichromated Gelatin for the Fabrication of Holographic Optical Elements," Appl. Opt. 18, 2407 (1979).
- S. P. McGrew, "Color Control in Dichromated Gelatin Reflection Holograms," SPIE Proc. 215, 24 (1980).

Received September 10, 1981; revised December 9, 1981

LeRoy D. Dickson and Albert D. Wolfheimer are located at the IBM Communication Products Division laboratory, Research Triangle Park, North Carolina 27709. Glenn T. Sincerbox is located at the IBM Research Division laboratory, 5600 Cottle Road, San Jose, California 95193.